HHS Public Access

Author manuscript

Chem Eng J. Author manuscript; available in PMC 2023 August 01.

Published in final edited form as:

Chem Eng J. 2022 August 01; 441: . doi:10.1016/j.cej.2022.135808.

pH Responsive Antibacterial Hydrogel Utilizing Catechol–Boronate Complexation Chemistry

Bo Liu[a], **Jianghua Li**[b], **Zhongtian Zhang**[a], **James D. Roland**[a], **Bruce P. Lee**[a,*]

[a]Department of Biomedical Engineering, Michigan Technological University, Houghton, Michigan 49931, United States

[b]Hunan Key Laboratory of Micro & Nano Materials Interface Science, College of Chemistry and Chemical Engineering, Central South University, Changsha 410083, China

Abstract

Bacteria such as Methicillin-resistant *Staphylococcus aureus* (MRSA) causes acidic microenvironment during infection. A biomaterial that exhibits tunable antimicrobial property in a pH dependent manner is potentially attractive. Herein, we presented a novel antibacterial hydrogel consisting of pH responsive and reversible catechol–boronate linkage formed between intrinsically bactericidal chlorinated catechol (catechol-Cl) and phenylboronic acid. Fourier transformed infrared spectroscopy (FTIR), oscillatory rheometry, and Johnson Kendall Roberts (JKR) contact mechanics testing confirmed the formation and dissociation of the complex in a pH dependent manner. When the hydrogel was treated with an acidic buffer (pH 3), the hydrogel exhibited excellent antimicrobial property against multiple strains of Gram-positive and negative bacteria including MRSA (up to 4 $\log_{10}$ reduction from 10^8 colony forming units/mL). At an acidic pH, catechol-Cl was unbound from the phenylboronic acid and available for killing bacteria. Conversely, when the hydrogel was treated with a basic buffer (pH 8.5), the hydrogel lost its antimicrobial property but also became non-cytotoxic. At a basic pH, the formation of catechol-boronate complex effectively reduce the exposure of the cytotoxic catechol-Cl to the surrounding. When further incubating the hydrogel in an acidic pH, the reversible complex dissociated to re-expose catechol-Cl and the hydrogel recovered its antibacterial property. Overall, the combination of catechol-Cl and phenylboronic acid provide a new strategy for designing hydrogels with pH responsive antibacterial activity and reduced cytotoxicity.

Graphical Abstract

*Correspondence author: Bruce P. Lee, bplee@mtu.edu.

Declaration of Competing Interest

The authors declare that they have no known competing financial interests or personal relationships that could have appeared to influence the work reported in this paper.

Appendix A. Supplementary data

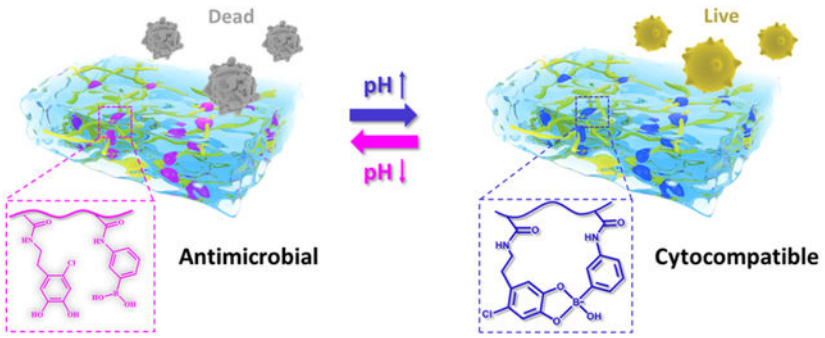

Keywords

antibacterial; halogenated catechol; catechol–boronate complexation; pH responsive; attenuated cytotoxicity

1. Introduction

Infection associated with antibiotic resistant bacteria has become a significant public health problem and is a significant economic burden for the infected patients[1–3]. Over reliance on antibiotics and frequent dosing are one of the main causes for the development of these drug resistance bacteria strains[4, 5]. As such, there is a need to find alternative antimicrobial agents. Phenols and halogenated phenols have been demonstrated to exhibit excellent antibacterial properties in recent decades.[6–8] Various chlorinated phenolic compounds, such as triclosan, chloroxylenol and hexachlorophene, are widely employed as disinfectants and antiseptics. The antibacterial mechanism of these phenolic compounds largely depends on their chemical structures. These phenolic compounds can damage bacterial cell membranes, thereby killing the bacteria by inducing leakage of intracellular components[9]. However, the cytotoxicity of these phenolic compounds is usually high due to the formation of electrophilic metabolites that may bind and damage DNA.

Catechol is a phenolic compound found in mussel adhesive proteins, plants, and fruits. Although catechol has predominantly been used as an adhesive molecule and a crosslinking precursor[10–12], catechol has been recently utilized as an antimicrobial agent[13, 14]. Catechol oxidation releases reactive oxygen species (ROS) as a byproduct, which has been demonstrated to function as an effective, broad-spectrum disinfectant[15–17]. When catechol is further modified with halogens such as chlorine, bromine and iodine, halogenated catechol exhibited excellent antibacterial property against multiple strains of drug resistance bacteria, including vancomycin resistant *enterococci* (VRE), antibiotic resistant *Pseudomonas aeruginosa* (PAER), antibiotic resistant *Acinetobacter baumannii* (AB) and carbapenem resistant *Klebsiella pneumoniae* (CRKP)[18]. The antibacterial ability of halogenated catechol is potentially due to its ability to inhibit bacterial fatty acid synthesis at the enoyl-acyl carrier protein reductase (FabI) step[18]. However, similar to other halogenated phenols, halogenated catechol is cytotoxic to mammalian cells. Moreover, the irreversible oxidation of catechol results in reduced antibacterial activity[19].

Bacterial metabolism and infection could induce unique microenvironment with pH differences, which can be utilized to develop pH responsive biomaterials to eradicate bacteria. Bacteria fermentation of sugar produces lactic acid, which can acidify its surroundings down to a pH as low as 3.5[20]. Similarly, Methicillin-resistant *Staphylococcus aureus* (MRSA) causes bloodstream infections that is five times more lethal than other strains, and the pH values of MRSA infection could decrease to ~5.5 or even lower[21]. Therefore, smart antibacterial systems were engineered to reduce systematic toxicity while release the bactericidal agents at lower an acidic pH[22, 23].

To reduce the cytotoxicity of halogenated catechol while preserving its antibacterial property, we incorporated phenylboronic acid as a temporary protecting group to create a pH responsive hydrogel. Catechol-boronate complex forms by the condensation between catechol and boronic acid at an basic pH and the complex dissociates at an acidic pH[24–26]. Due to its reversible and dynamic nature, their corresponding polymers are applied in tunable smart adhesives[27, 28], pH responsive drug carriers[29, 30], and self-healing hydrogels[31]. Here, we seek to test the hypothesis that the pH-dependent nature of the catechol-boronate complex could be used to control the antimicrobial property and cytotoxicity of halogenated catechol. At a basic pH, catechol-boronate complexation is expected to reduce the cytotoxicity of the halogenated catechol. When the complex dissociates in an acidic pH, the halogenated catechol would be exposed for enhanced antimicrobial activities.

We incorporated both chlorinated catechol (catechol-Cl) and phenylboronic acid into a hydrogel to create a pH responsive, antimicrobial biomaterial with improved cytotoxicity. The hydrogel was formed by copolymerizing catechol-Cl-containing monomer, 6-chlorodopamine methacrylamide (DMA-Cl), and 3-acrylamido phenylboronic acid (AAPBA). The reversible nature of the catechol-boronate complex was confirmed by Fourier transformed infrared spectroscopy (FTIR), field emission scanning electron microscope (FE-SEM), oscillatory rheometry, and Johnson Kendall Roberts (JKR) contact mechanic test. The antibacterial property of the hydrogels against different bacterial strains, including Gram-positive (*S. aureus* and MRSA) and Gram-negative (*Pseudomonas aeruginosa* and *Escherichia coli*) bacteria, was investigated at different pH levels. Additionally, the effect of pH on the cytotoxicity of hydrogels containing catechol-Cl and phenylboronic acid against human skin fibroblast (HSF) was evaluated.

2. Materials and methods

2.1. Materials

N-Hydroxyethyl acrylamide (HEAA), dopamine hydrochloride, methacryloyl chloride, AAPBA, N,N'-methylenebisacrylamide (MBAA), azobisisobutyronitrile (AIBN), N-chlorosuccinimide (NCS), trifluoroacetic acid (TFA), triethylamine (TEA), methanol, trishydroxymethyl aminomethane (Tris), 3-[4, 5-dimethylthiazoyl-2-yl]-2, 5-diphenyl tetrazolium bromide (MTT), hydrogen chloride (HCl) solution (37 wt%), sodium chloride (NaCl), 4', 6-diamidino-2-phenylindole dihydrochloride (DAPI) and dimethyl sulfoxide (DMSO) were all purchased from Sigma-Aldrich. Sodium sulfate (Na_2SO_4), ethyl acetate (EA) and hexane were purchased from Fisher Scientific Co. All the bacteria were

purchased from American Type Culture Collection (ATCC). HSF cells were purchased from Honsunbio. Ltd. (Shanghai, China). Lysogeny Broth (LB) agar medium, Mueller Hinton Broth medium (MHB), phosphate buffer saline (PBS), Calcein-AM/PI, LIVE/DEAD Bac Light Bacterial Viability Kit were purchased from Thermo Fisher Scientific. The acidic solution was prepared by titrating a 0.1 M NaCl solution to pH 3 using 1 M HCl, while the basic buffer medium was prepared by titrating 10 mM Tris with 1 M HCl to pH 8.5. Other reagents were used as received without further purification. DMA was prepared using previously published protocol[18].

2.2. Synthesis of DMA-Cl

The two-step synthesis of DMA-Cl was prepared in one-pot. Dopamine hydrochloride (0.19 g, 1 mmol) and NCS (0.15 g, 1.1 mmol) was added to a 5 mL of TFA and the reaction mixture was stirred overnight at room temperature. TFA was removed by rotary evaporation. The viscous residue was dissolved in 10 mL of methanol and TEA (0.57 mL, 4 mmol) was added. Methacryloyl chloride (0.16 mL, 1.5 mmol) in EA (5 mL) was slowly added. The solution was stirred for 3 h under nitrogen atmosphere. After removing the solvent, the residue was extracted with EA (50 mL) and washed twice with 1 M HCl. After that, the organic phase was further washed with brine and dried with Na_2SO_4. The solution was concentrated under reduced pressure to yield the crude solid. The product was purified by silica gel column chromatography using a EA/hexane mixture (v:v = 60:40, R_f = 0.55) to afford the product (0.14 g, 51.5%) as a grey solid. ^{1}H NMR (400 MHz, DMSO-d_6): δ (ppm) = 9.15 (br, 2H, Ph-OH), 7.97 (t, 1H, -NH), 6.71 (s, 1H, Ph-H), 6.61 (s, 1H, Ph-H), 5.61 (s, 1H, =CH_2), 5.29 (s, 1H, =CH_2), 1.83 (s, 3H, -CH_3).

2.3. Preparation of pH responsive hydrogels

Hydrogels were prepared by curing a precursor solution containing 1 M of HEAA with 10 mol% of DMA or DMA-Cl, 10 mol% of AAPBA, 4 mol% of MBAA and 1 mol% of AIBN dissolved in 50% (v/v) DMSO in deionized (DI) water. HEAA polymerized to form a hydrophilic and biocompatible polymer network [32]. MBAA is a commonly used crosslinker for forming crosslinked hydrogels [33, 34] and AIBN is a commonly used thermal initiator for free-radical polymerization [35]. The precursor solution was added to a glass mold with a spacer (length × width × thickness = 5 cm × 5 cm × 0.2 cm) and incubated at 80 °C for 3 h. The hydrogels were washed by submerging in an aqueous solution (pH 3) with gentle nutation and frequent medium changes. Depending on the monomer compositions in the hydrogels, five hydrogel formations were prepared: (i) poly(HMAA-*co*-MBAA) hydrogel (HM); (ii) poly(HMAA-*co*-MBAA-*co*-DMA) hydrogel (HMD); (iii) poly(HMAA-*co*-MBAA-*co*-DMA-*co*-AAPBA) hydrogel (HMDA); (iv) poly(HMAA-*co*-MBAA-*co*-DMA-Cl) hydrogel (HMDc); (v) poly(HMAA-*co*-MBAA-*co*-DMA-Cl-*co*-AAPBA) hydrogel (HMDcA).

2.4. Material characterization

Fourier transformed infrared spectroscopy (FTIR) was performed using Shimadzu IRTracer-100 spectrometer. Hydrogels for were incubated in pH 3, 7.4, 8.5 or 9 for 24 h and dried under the vacuum for 48 h. To image the network morphology, hydrogels were freeze-dried, coated with platinum, and imaged using a FE-SEM (HITACHI S-4700). To

determine the swelling ratio (SR) of the hydrogels, lyophilized samples were incubated in pH 3, 8.5 and 9 at 25 °C for up to 24 h. The mass of hydrogels in the swollen (W_s) and dried (W_d) states was used to determine the SR as calculated by: $SR = (W_s - W_d)/W_d \times 100\%$. To determine the mechanical properties, hydrogel samples (diameter = 7 mm; thickness = 3 mm) were subjected to amplitude sweep experiment (0.01–100 % strain, frequency = 0.1 Hz) using an oscillatory rheometer (HR-2, TA Instruments) to determine the storage (G') and loss (G") moduli. The samples were tested using a parallel plate set up with a gap distance that was 87.5% of the measured thickness of each sample. The thickness of the hydrogel was measured using a digital Vernier caliper before testing. Unconfined, uniaxial compression testing was performed using a mechanical test instrument (ElectroForce 3200 Series III, Bose Corporation). Hydrogels (n = 3) were compressed at a rate of 0.05 mm/s until the sample fractured. The dimensions of each hydrogel (diameter = 7 mm; thickness = 3 mm) were measured using a digital caliper immediately before testing. Stress was determined based on the measured load divided by the initial surface area of the sample. Strain was determined by dividing the change in the position of the compressing plate by the initial thickness of the hydrogel. Toughness was determined by the integral of the stress-strain curve. The elastic modulus was taken from the slope of the stress-strain curve between a strain of 0.05 and 0.15.

2.5. JKR Contact mechanic test

JKR contact mechanic test was used to evaluate the pH-dependent adhesive property of the hydrogel using published protocols [27]. Contact mechanics tests were conducted using hemispherical-shaped hydrogel using a custom-built indentation device consisted of a 10-g load cell (Transducer Techniques), a high-resolution miniature linear step motor (MFA-PPD, Newport), and an indenter (ALS-06, Transducer Techniques). Hemispherical hydrogel samples were attached to the indenter using superglue (Gorilla Super Glue) and brought into contact to a borosilicate glass surface wetted with 25 μL of buffer solution. The buffer solution was kept being the same as the solution last used to equilibrate the sample. The hemispherical hydrogels were compressed at a rate of 1 μm/s until the maximum preload of 20 mN was reached. After reaching the maximum preload, the samples were retracted immediately at the same rate of 1 μm/s. The tensile force was measured and recorded from the time that the sample began compressing up until the sample was retracting and the measured tensile force returned to a 0 mN reading. The maximum adhesive force (F_{max}) and the work of adhesion (W_{adh}) were determined following previously published protocols[27].

Two different experiments were performed to evaluate the rate of catechol-boonate complex formation and dissociation based on the time it took for the F_{max} and W_{adh} to change with changing pH. In the first experiment, hydrogels were first incubated in 1 mL of pH 3 solution for 24 h followed by incubation in 1 mL of pH 8.5 or 9 tris buffer solution for varying amount of time (5, 10, 15, and 20 min) prior to testing. In the second experiment, samples were equilibrated in 1 mL of pH 3 solution for 24 h, 1 mL of pH 8.5 or 9 tris buffer solution for a specified time (5, 10, 15, and 20 min), and then 1 mL of pH 3 solution for up to 48 h before testing. All samples were equilibrated with gentle nutation.

2.6. Antibacterial property of hydrogels

Three antibacterial tests were performed using hydrogel discs (diameter = 0.7 cm; thickness = 0.3 cm) equilibrated at different pH levels. In the first test, hydrogels were equilibrated in pH 3 solution for 24 h to test the antimicrobial property of the exposed catechol. In the second test, hydrogels were equilibrated in pH 3 solution for 24 h and then pH 8.5 or pH 9 tris buffer solution for 12 h to evaluate the antimicrobial property of the catechol-boronate complex. In the last test, hydrogels were equilibrated in pH 3 solution for 24 h, then pH 8.5 or pH 9 tris buffer solution for 12 h, and then of pH 3 solution for 12 h to examine the recovery of the free catechol and its antimicrobial property. Before incubation with bacteria, the hydrogels were washed with PBS buffer (pH 7.4) for several times to excess acidic or basic buffer. PBS was used as the control and was directly added to the bacterial suspension. *E. coli* ATCC8739, *S. aureus* ATCC29213, MRSA (BAA40), and *P. aeruginosa* (PAO1) were inoculated and dispersed in 4 mL MHB at 37 °C with continuous shaking to mid log phase (~10^8 CFU/mL). 10 μL of bacterial suspension was spread onto the surface of the samples, which were further incubated at 37 °C for 24 h to inoculate the bacteria. Samples were transferred to vessels containing 1 mL PBS and vortexed to obtain bacterial suspensions. The suspension was diluted and plated on LB agar. The agar plates were incubated at 37 °C for 24 h. The colony forming unit (CFU) number was counted and expressed in killing efficiency: [(cell count of control - survivor count on sample)/cell count of control] × 100%.

2.7. Morphology of hydrogel-treated MRSA

MRSA BAA40 were grown in MHB (4 mL) at 37 °C with continuous shaking to mid log phase and washed twice with PBS and then diluted to 10^5–10^6 CFU/mL in MHB. 100 μL of bacterial suspension was spread onto the surface of pH treated hydrogels, which were further incubated at 37 °C for 24 h. After incubation, bacteria on the surface of hydrogels were fixed using 2.5% glutaraldehyde at 4°C overnight followed by dehydration by air drying for 72 h. The dehydrated sample was coated with platinum and imaged using FE-SEM.

2.8. Cytotoxicity of hydrogels

Cytotoxicity of hydrogel discs (diameter = 0.7 cm; thickness = 0.3 cm) were evaluated after exposing them to three different incubation protocols. Hydrogels were first equilibrated in pH 3 solution for 24 h to evaluate the cytotoxicity of the exposed catechol. Next, hydrogels were equilibrated in pH 3 solution for 24 h and then pH 8.5 (HMDc and HMDcA) or pH 9 (HM, HMD and HMDA) tris buffer solution for 12 h to examine the cytotoxicity of the catechol-boronate complex. Lastly, hydrogels were equilibrated in pH 3 solution for 24 h, then pH 8.5 (HMDc and HMDcA) or 9 (HM, HMD and HMDA) tris buffer solution for 12 h, and then of pH 3 solution for 12 h to examine the recovery of the free catechol and its. After that, all the hydrogels were washed with PBS buffer (pH 7.4) to remove the remaining acidic or basic buffer. The washed hydrogels were immersed in 5 mL of PBS for 24 h with gentle nutation. After that, 100 μL of the hydrogel extractions were mixed with 100 μL of 10^5 cells/well HSF cell suspension (cultured in Dulbecco's Modified Eagle Medium containing 10% fetal bovine serum and 1% penicillin-streptomycin) in a 96-well plate and incubated at 37 °C in 5% CO_2 atmosphere for 24 h. After 10 μL of 10% cell counting kit-8 solution was added to each well, the cells were further incubated for additional 1 h.

Subsequently, the plate was subjected to measurement of OD at 450 nm using a microplate reader (Infinite F50). PBS was used as the blank control. OD values were measured at 570 nm using Infinite F50 TECAN plate reader (TECAN, Swiss). Cell viability was calculated based on the following equation: Cell viability (%) = $OD_{hydrogel}$ well/$OD_{control}$ well × 100%.

2.9. Live cell imaging assay

HSF cells were cultured with hydrogel extraction solutions (pH 3, 7.4 and 8.5) in a 24-well plate (10^4 cells/well) for 24 h. After that, the medium was removed and washed with 1X PBS buffer to remove unattached cells. After the washing procedure, 2 mL 4 % paraformaldehyde in PBS was added into each well for 15 min to fixed cells, and the cells were washed with 1X PBS buffer three times. Then 1 mL 1 % BSA was added into each well to incubate at 37 °C for 30 min. BSA was removed and washed by 1X PBS buffer. Finally, diluted rhodamine phalloidin (100 μL, 1 μg/mL) was added into each well for 1 h and DAPI (100 μL, 0.5 μg/mL) was added into each well for 3 min, respectively. The cell morphology was observed by a Live Cell Imaging System (Zeiss Cell Observer).

3. Results and discussion

3.1. Preparation of hydrogels

DMA-Cl was synthesized in one-pot (Scheme S1) to create a polymerizable monomer containing a chloro-functionalized catechol side chain. ^{1}H NMR confirmed the structure of DMA-Cl (Figure S1). DMA-Cl contains a chloride atom at the 6-position of the catechol phenol structure as opposed to a hydrogen in DMA (Figure 1). Hydrogels were prepared using either DMA or DMA-Cl by thermal-initiated free radical polymerization with or without a phenylboronic acid-containing monomer, AAPBA. The stability of boronate ester bond depend on acid dissociation constants (pKa) of catechol and boronic acid[36, 37]. The ideal complexation pH between a diol and a boronic acid is the average of their respective acid pKa values ($pH_{ideal} = (pKa_{diol} + pKa_{acid})/2$)[38]. The pKa of chlorinated catechol (catechol-Cl), catechol and boronic acid are 8.3, 9,2, and 8.8, respectively[38, 39]. Therefore, pH 8.5 ($pKa_{catechol\text{-}Cl} + pKa_{boronic\ acid}/2$) and pH 9 ($pKa_{catechol} + pKa_{boronic\ acid}/2$) were chosen to study the formation of catechol-boronate complexation for hydrogels containing DMA-Cl and DMA, respectively. pH 3 was chosen to maintain the dissociated and reduced form of catechol.

FTIR spectra confirmed the composition of the hydrogels (Figure 2). All hydrogels exhibited C=O stretching peak at 1640 cm^{-1}, confirming the presence of amide bond found in HEAA and MBAA. Catechol-containing hydrogels exhibited C-H bending peaks associated with benzene rings at 500–600 cm^{-1}. Spectra of DMA-Cl-containing hydrogel (HMDc) contain a characteristics peak at 826 cm^{-1}, which was attributed to C-Cl stretching (Figure 2b). HMDA and HMDcA are modified with both catechol (DMA and DMA-Cl, respectively) and phenylboronic acid moieties and exhibited a new peak at around 1485 cm^{-1} at pH 8.5 and 9, respectively, confirming catechol-boronate complexation at a basic pH (Figure 2c). In contrast, the peak disappeared at pH 3 and 7.4 (Figure 2d). It indicated that the catechol-boronate complex dissociated with decreasing pH.

Optical images of these hydrogels after incubation at different pH are shown in Figure 3a. The catechol-free HM did not demonstrate any color change when incubated at different pH. The color of HMD and HMDc was changed from colorless at pH 3 to dark red at pH 9 and 8.5, respectively, as a result of catechol oxidation in the absence of phenylboronic acid. For HMDA and HMDcA, the color change not as discernable after incubating at a basic pH. The presence of boronic acid minimized catechol oxidation at elevated pH levels. The swelling ratio of HM was around 15 and did not change with pH. At pH 3, incorporating catechol (HMD and HMDc) and both catechol and phenylboronic acid (HMDA and HMDcA) progressively reduced swelling ratio. Catechol and catechol-Cl and phenylboronic acid contain a hydrophobic benzene ring which reduced the swelling ratio of the hydrogel. Additionally, these molecules can participate in intermolecular interactions such as **π–π** interaction or hydrogen bonding, which contributed to hydrogel deswelling[33]. However, the swelling ratios of HMDA and HMDcA increased from around 6 at pH 3 to over 26 at elevated pH values (Figures 3b). Similarly, SEM images of the cross-section of HMDA and HMDcA incubated at basic pH also exhibited pores that were 5 times larger than those at pH 3 (Figure 4), which corroborated with the obtained swelling ratio values. Both increase in the extent of swelling and pore size are attributed to the repulsion of the negatively charged catechol-boronate complexes formed at the ideal complexation pH[27].

3.2. Viscoelasticity of hydrogels

All the hydrogels exhibited linear elasticity, where G' were independent of applied strain between 0.1 to 100% (Figure S3 and Figure 5). Additionally, G' values were higher than those of G", indicating that the hydrogels were chemically crosslinked. G' values of the catechol-free hydrogel (HM) did not change with changing pH. In contrast, catechol-containing hydrogels (HMD, HMDc, HMDA, and HMDcA) exhibited higher G' at pH 9 and 8.5 in the elastic ranges when compared to those at pH 3. The increased stiffness is attributed to catechol's ability to form intermolecular interactions and crosslinkings [27, 40]. For hydrogels that contains both catechol and phenylboronic acid (HMDA and HMDcA), G" values at a basic pH were one order of magnitude higher than those measured at pH 3. This increase in G" value corresponds to increased viscous dissipation and the formation of reversible physical interaction in the hydrogel network attributed to catechol-boronate complexation. Similarly, HMDA and HMDcA exhibited a significantly increase in the maximum stress and toughness (2.5–3 fold increase) when incubated at a basic pH based on compression testing results (Figure S4 and Table S1). Most notably, these hydrogels did not fracture even when they were compressed to the maximum load of the load cell. This indicated that the formation of the reversible catechol-bronate complex introduced sacrificial bonds within the hydrogel network, which likely dissipated fracture energy during mechanical loading [41, 42].

3.3. pH responsive behavior of hydrogels

To evaluate the pH-responsive behavior of the catechol-boronate complex, JKR contact mechanics tests were performed to determine the reversibility of the catechol-boronate complex under acidic and basic conditions based on the adhesive contacts between the hydrogels and a borosilicate glass surface (Figure S5). In the dissociated form, both the catechol and the phenylboronic acid can contribute to strong interfacial binding through

hydrogen bonding, hydrophobic and electrostatic interaction[27]. Hence, HMDA and HMDcA exhibited high F_{max} and W_{adh} (13.26 mN and 526.18 mJ/m^2, respectively, for HMDA and 11.70 mN and 492.71 mJ/m^2, respectively, for HMDcA) at pH 3 when catechol and phenylboronic acid are in their dissociated form (Figure 6). However, when incubated in pH 9, HMDA rapidly reduced its adhesive property within 5 min through the formation of catechol-boronate complex. On the other hand, the adhesive property of HMDcA required at least 15 min of incubation at pH 8.5 to reduce its adhesive property. Nevertheless, HMDA and HMDcA recovered around 80% of its original F_{max} and W_{adh} values after 48 h incubation at pH 3 (Figure 7 and Figure S6). These results indicated that the formation of catechol-boronate complexes occurred at a faster rate (5–20 min) when compared to the dissociation of the complex (~48 h). Additionally, the adhesion data indicated that catechol-Cl exhibited the ability to form reversible complex with phenylboronic acid in a pH dependent manner similar to unmodified catechol. However, the complexes did not completely dissociate with changing pH as HMDcA did not fully recover its original adhesive property even after 48 h of incubation in an acidic pH. This is potentially due to the bulky phenyl functional group that is linked to the boron center, which enhances the stability of the catechol-boronate complex[43].

3.4. Antibacterial activity of pH responsive hydrogel

Antibacterial activity of hydrogels against both Gram-positive (*S. aureus* and MRSA) and Gram-negative (*E. coli* and PAO1) bacteria was tested after the samples were incubated at different pH (Figure 8 and Figure S7). At pH 3, all the catechol containing hydrogels (HMD, HMDc, HMDA and HMDcA) exhibited over 90% antibacterial efficacy, while the control hydrogel without catechol (HM) did not exhibit any antibacterial activity. The unmodified catechol (HMD and HMDA) achieved a 1 $\log_{10}$ reduction, while hydrogels containing catechol-Cl (HMDc and HMDcA) exhibited 3–4 $\log_{10}$ reduction. This is in agreement with previously published work where halogenated catechol exhibited significantly better antimicrobial property when compared to unmodified catechol (2 orders of magnitude difference in the CFU count) [18]. This is potentially due to halogenated catechol's ability to form strong complex with FabI and thus causing bacterial cell death through disintegration of its cellular membrane, similar to the antimicrobial mechanism of other chlorinated phenolic compounds such as triclosan [44, 45]. After incubation at a basic pH, HMD and HMDc still retain around 90% killing efficiencies (1 $\log_{10}$ reduction) when compared with acid treated gel, indicating that the oxidized form of catechol, benzoquinone, exhibited some level of antibacterial property[46, 47]. In contrast, phenylboronic acid-containing HMDA and HMDcA lost their antibacterial activity at a basic pH and resulted in less than 1 $\log_{10}$ reduction of bacterial CFU (Figure 8b). The formation of catechol-boronate complex at a basic pH rendered the catechol-Cl less accessible for antimicrobial activity.

When the pH was changed back to pH 3, HMDcA exhibited the highest antibacterial activity among all the hydrogel formulations tested (Figure 8c). HMDcA exhibited over 99 % killing efficiency (>2 $\log_{10}$ reduction) towards all four strains of bacteria. When HMDcA was re-exposed to an acidic pH, the catechol-boronate complex dissociated and re-exposed catechol-Cl for antimicrobial activity. Additionally, the phenylboronic acid acted as the temporary protecting group that minimized oxidation of catechol-Cl during the treatment

at basic condition. However, the antimicrobial activity of the re-exposed catechol-Cl was notably lower when compared to the first pH 3 incubation cycle (> 99.9% killing efficiency; Figure 8a). It is possible that catechol-boronate complex did not completely dissociate, which corroborates with the JKR results that indicated around 80% adhesion strength recovery after second pH 3 treatment (Figure 7b). On the other hand, hydrogels without phenylboronic acid (e.g., HMDc) did not result in an increase in antimicrobial activity even after the second pH 3 treatment. Catechol-Cl likely oxidized irreversibly during multiple cycles of base and acid treatment[27]. These results indicated that the catecholic form is responsible for strong antimicrobial activity and the importance of phenylboronic acid in functioning as the temporary protecting group in preventing catechol oxidation. Finally, hydrogel containing both the unmodified catechol and phenylboronic acid (HMDA) also demonstrated pH responsive antibacterial activity. However, HMDA exhibited much poorer antimicrobial potency (1 $\log_{10}$ reduction) at an acidic pH when compared to HMDcA.

A suspension containing MRSA was applied over the surface of the hydrogel samples and the cellular morphology after 24 h incubation was observed using FE-SEM. When MRSA was applied over the non-bactericidal HM hydrogel, the bacteria remained smooth and round in shape with elevated bacteria count (Figure S8). However, there was a drastically reduction in cell count when MRSA was applied over HMDc regardless of pH (Figures 9a–9c). Additionally, these cells exhibited morphological change and deformation suggesting that MRSA was killed by the membrane disruption mechanism. In contrast, MRSA incubated on HMDcA exhibited pH-dependent antimicrobial property. MRSA exposed to pH 3-treated HMDcA demonstrated a drastic reduction in MRSA count and cell deformation (red arrows, Figure 9d). Basic solution treated HMDcA was not antimicrobial and MRSA count was high with no obvious change in morphology when compared to MRSA applied over non-bactericidal HM hydrogel (Figure 9e). When HMDcA was further incubated in pH 3, the antibacterial ability was recovered (Figure 9f). Overall, FE-SEM images corroborated with the antibacterial results based on CFU counting and HMDcA exhibited pH responsive antibacterial activity.

3.5. Cytotoxicity of hydrogels

MTT assay was used to evaluate the cytotoxicity of hydrogels (Figure 10). Catechol-free HM hydrogels exhibited cell viability above 90%. When DMA and DMA-Cl were copolymerized into the hydrogels, the cell viability of HMD and HMDc was drastically reduced to around 70 and 40%, respectively, and cell viability did not vary with changing pH. This reduction in cell viability was attributed to the toxicity of catechol [48] and benzoquinone [49], which would induce cell death by apoptosis. Specifically, catechol-Cl was highly cytotoxic when compared to that of the unmodified catechol. When phenylboronic acid was incorporated into the hydrogels, both HMDA and HMDcA exhibited pH dependent cycotoxicity. When HMDA and HMDcA was incubated at basic pH prior to cytotoxicity test, the cell viability increased to over 75%. This indicated that the formation of catechol-boronate complex drastically reduced the cytotoxicity of catechol and catechol-Cl. After catechol-boronate complexes were dissociated again at pH 3, cell viability decreased again. These results suggest that catechol-boronate complexation can be used to attenuate the cell cytotoxicity of catechol. The morphology of HSF cell incubated with the

extracts of HM and HMDcA was determined by the living cell imaging assay (Figure S9). For the cells treated with the extracts of HM, the number of the HSF cells were profuse and the nuclear structure were clear. These HSF also exhibit the spindlelike morphology. In contrast, much fewer HSF cells were observed for cells exposed to HMDcA at pH 3, potentially due to the cytotoxic nature of the catechol-Cl. When HMDcA was incubated at elevated pH levels, there was an increase in cellular density.

4. Discussion

Taken together, both catechol-Cl and phenylboronic acid moieties were utilized to create a pH responsive, antimicrobial hydrogel. Catechol-Cl formed a complex with phenylboronic acid in a similar pH dependent manner as that of unmodified catechol. The formation and dissociation of the catechol-boronate complex was confirmed by FTIR spectroscopy (Figure 2), oscillatory rheometry (Figure 5), and JKR contact mechanics test (Figure 7). Catechol-Cl is inherent antimicrobial and its antimicrobial property stem from its ability to disrupt bacterial cellular membrane through binding to the enzyme, FabI, that is critical to fatty acid synthesis[18]. At an acidic pH, catechol-Cl is dissociated from phenylboronic acid and is available for interacting with bacteria, which resulted in enhanced antimicrobial property (Figure 8). Additionally, catechol-Cl-containing hydrogel was effective against both Gram-positive and Gram-negative bacteria, including the drug resistant strain, MRSA. However, catechol-Cl was also significantly more cytotoxic when compared to that of unmodified catechol (Figure 10), which necessitated the incorporation of phenylboronic acid as a temporary protecting group to attenuate its cytotoxicity. Complexation between catechol-Cl and phenylboronic acid reduced the availability of catechol-Cl, thus reducing the cytotoxicity of the hydrogel. Additionally, the presence of phenylboronic acid prevented irreversible oxidation of catechol-Cl while preserving its antimicrobial property.

Although hydrogels reported here demonstrated potential in functioning as a novel biomaterial with tunable antimicrobial property, there are still several issues needed to be addressed. Formation of catechol-boronate complex significantly increased the extent of swelling (5 fold increase in swelling ratio), which could be problematic if the hydrogel was used as an implant. Excessive swelling could result in elevated compression on neighboring tissues[50, 51]. However, extensive swelling did not compromise the mechanical integrity of these hydrogel and catechol-boronate complexation significantly enhance the toughness of these hydrogels. The elevated swelling was a result of charge repulsion between negatively charged catechol-boronate complexes within the hydrogel network[27], and oppositely charged cationic functional groups could be incorporated to neutralize the charged polymer network. Additionally, incorporation of charged functional groups could be utilized to tune the complexation pH[52], which could reduce the need for elevated pH for forming the complex. Although the formation of the catechol-boronate complex occurred relatively quickly (< 15 min), the dissociation of the complex could not be completely achieved even after 48 h of incubation in an acidic buffer. Additional work is needed to increase the rate of the complex dissociation in order to fully recover the antibacterial potency of catechol-Cl. This can potentially be achieved by controlling the reactivity of the boronic acid used as the temporary protecting group[43]. Finally, degradable linkages such as hydrolysable ester bonds could be incorporated to create hydrogels that are biodegradable.

Nevertheless, a pH responsive, antimicrobial biomaterial that can adapt to the acidic environment created by bacteria is attractive. In an acidic environment that is associated with bacteria fermentation of sugar and infection[20, 21], catechol-Cl is unbound and available to achieve the desired antimicrobial property. Catechol-boronate complexation formed at an elevated pH to minimize the cytotoxicity of catechol-Cl. Unlike antimicrobial catechol-based hydrogels reported by others[53, 54], the antibacterial property of the catechol-based hydrogel reported here could be reversibility turned “on” and “off” in response to changes in pH in its surrounding. This enables the hydrogel to perform the antimicrobial function on demand and “hide” the cytotoxic catechol-Cl when its function is no longer needed (i.e., when the infection has resolved). To date, most of the existing pH responsive antibacterial hydrogels or polymers are cationic[55–57], which bind to and disrupt the negatively charged bacterial membranes. However, the exposed cationic moieties are also toxic to mammalian cells[58]. Therefore, a pH responsive system should be engineered to reduce toxicity at physiological pH, while retaining its bactericidal effect at a low pH[22, 23]. Additionally, the antibacterial property of the catechol-Cl-containing hydrogel was derived from the intrinsic antibacterial property of the catechol-Cl itself rather than the loading drugs or antibiotics[59], which will prolonged its antimicrobial property. The combination of halogenated catechol and boronic acid provides a new strategy for designing a novel pH responsive and inherent antibacterial hydrogel with improved biocompatibility.

4. Conclusion

In conclusion, chloro-functionalized catechol was incorporated into a hydrogel along with phenylboronic acid. FTIR, swelling behavior, FE-SEM and JKR contact mechanics test confirmed the pH responsive catechol-boronate complex formation and dissociation. Formation of the complex drastically increased the mechanical property of the hydrogel. By controlling the complexation behavior using pH, it is feasible to tune the antimicrobial property and cytotoxicity of the hydrogel reversibly.

Supplementary Material

Refer to Web version on PubMed Central for supplementary material.

Acknowledgment

This work was supported by the National Institutes of Health [grant number R15GM135875 (B.P.L.)]; the Office of Naval Research [grant number N00014-20-2230 (B.P.L.)]; the Office of the Assistant Secretary of Defense for Health Affairs through the Defense Medical Research and Development Program [grant number W81XWH181061 (B.P.L.)]; and the National Science Foundation [grant number DMR 2001076 (B.P.L.)].

ReferencesUncategorized References

[1]. Sugden R, Kelly R, Davies S, Combatting antimicrobial resistance globally, Nature Microbiology 1(10) (2016) 16187.

[2]. Nathwani D, Raman G, Sulham K, Gavaghan M, Menon V, Clinical and economic consequences of hospital-acquired resistant and multidrug-resistant Pseudomonas aeruginosa infections: a systematic review and meta-analysis, Antimicrobial Resistance and Infection Control 3(1) (2014) 32. [PubMed: 25371812]

[3]. Morales E, Cots F, Sala M, Comas M, Belvis F, Riu M, Salvadó M, Grau S, Horcajada JP, Montero MM, Castells X, Hospital costs of nosocomial multi-drug resistant Pseudomonas aeruginosa acquisition, BMC Health Services Research 12(1) (2012) 122. [PubMed: 22621745]

[4]. Lindsay EN, Suzanne B, Richard C, Rice JC, Anthony S, Hooton TM, Infectious Diseases Society of America Guidelines for the Diagnosis and Treatment of Asymptomatic Bacteriuria in Adults, Clinical Infectious Diseases 40(5) (2005) 643–654. [PubMed: 15714408]

[5]. Davies D, Understanding biofilm resistance to antibacterial agents, Nature Reviews Drug Discovery 2(2) (2003) 114–122. [PubMed: 12563302]

[6]. Bouarab-Chibane L, Forquet V, Lanteri P, Clement Y, Leonard-Akkari L, Oulahal N, Degraeve P, Bordes C, Antibacterial properties of polyphenols: characterization and QSAR (quantitative structure activity relationship) models, Front. Microbiol 10 (2019) 23. [PubMed: 30740093]

[7]. Miklasinska-Majdanik M, Kepa M, Wojtyczka RD, Idzik D, Wasik TJ, Phenolic compounds diminish antibiotic resistance of Staphylococcus aureus clinical strains, Int. J. Env. Res. Pub. He 15(10) (2018).

[8]. Park E-S, Moon W-S, Song M-J, Kim M-N, Chung K-H, Yoon J-S, Antimicrobial activity of phenol and benzoic acid derivatives, Int. Biodeter. Biodegr 47(4) (2001) 209–214.

[9]. Lambert PA, Hammond SM, Potassium fluxes, first indications of membrane damage in micro-organisms, Biochem. Bioph. Res. Co 54(2) (1973) 796–9.

[10]. Pandey N, Soto-Garcia LF, Liao J, Philippe Z, Nguyen KT, Hong Y, Mussel-inspired bioadhesives in healthcare: design parameters, current trends, and future perspectives, Biomater Sci-Uk 8(5) (2020) 1240–1255.

[11]. Schmidt G, Woods JT, Fung LX-B, Gilpin CJ, Hamaker BR, Wilker JJ, Strong Adhesives from Corn Protein and Tannic Acid, Advanced Sustainable Systems 3(12) (2019) 1900077.

[12]. Wang Y, Jeon EJ, Lee J, Hwang H, Cho S-W, Lee H, A Phenol-Amine Superglue Inspired by Insect Sclerotization Process, Adv. Mat 32(43) (2020) 2002118.

[13]. Pinnataip R, Lee BP, Oxidation Chemistry of Catechol Utilized in Designing Stimuli-Responsive Adhesives and Antipathogenic Biomaterials, ACS Omega 6(8) (2021) 5113–5118. [PubMed: 33681552]

[14]. Razaviamri S, Wang K, Liu B, Lee BP, Catechol-Based Antimicrobial Polymers, Molecules 26(3) (2021) 559. [PubMed: 33494541]

[15]. Meng H, Forooshani PK, Joshi PU, Osborne J, Mi X, Meingast C, Pinnaratip R, Kelley JD, Narkar A, He W, Frost MC, Heldt CL, Lee BP, Biomimetic recyclable microgels for on-demand generation of hydrogen peroxide and antipathogenic application, Acta Biomater 83 (2019) 109–118. [PubMed: 30541699]

[16]. Forooshani PK, Polega E, Thomson K, Bhuiyan MSA, Pinnaratip R, Trought M, Kendrick C, Gao Y, Perrine KA, Pan L, Lee BP, Antibacterial Properties of Mussel-Inspired Polydopamine Coatings Prepared by a Simple Two-Step Shaking-Assisted Method, Frontiers in Chemistry 7(631) (2019).

[17]. Kord Forooshani P, Pinnaratip R, Polega E, Tyo AG, Pearson E, Liu B, Folayan T-O, Pan L, Rajachar RM, Heldt CL, Lee BP, Hydroxyl Radical Generation through the Fenton-like Reaction of Hematin- and Catechol-Functionalized Microgels, Chemistry of Materials 32(19) (2020) 8182–8194. [PubMed: 34334946]

[18]. Liu B, Zhou C, Zhang Z, Roland JD, Lee BP, Antimicrobial property of halogenated catechols, Chemical Engineering Journal 403 (2021) 126340. [PubMed: 32848507]

[19]. Suarez S, Dodd MC, Omil F, von Gunten U, Kinetics of triclosan oxidation by aqueous ozone and consequent loss of antibacterial activity: Relevance to municipal wastewater ozonation, Water Research 41(12) (2007) 2481–2490. [PubMed: 17467034]

[20]. Charlier C, Cretenet M, Even S, Le Loir Y, Interactions between Staphylococcus aureus and lactic acid bacteria: An old story with new perspectives, International Journal of Food Microbiology 131(1) (2009) 30–39. [PubMed: 18687499]

[21]. Weinrick B, Dunman PM, McAleese F, Murphy E, Projan SJ, Fang Y, Novick RP, Effect of mild acid on gene expression in Staphylococcus aureus, J. Bacteriol 186(24) (2004) 8407. [PubMed: 15576791]

[22]. Ye M, Zhao Y, Wang Y, Yodsanit N, Xie R, Gong S, pH-Responsive Polymer–Drug Conjugate: An Effective Strategy to Combat the Antimicrobial Resistance, Adv. Funct. Mater 30(39) (2020) 2002655.

[23]. Gao Y, Wang J, Chai M, Li X, Deng Y, Jin Q, Ji J, Size and Charge Adaptive Clustered Nanoparticles Targeting the Biofilm Microenvironment for Chronic Lung Infection Management, ACS Nano 14(5) (2020) 5686–5699. [PubMed: 32320228]

[24]. Pizer R, Babcock L, Mechanism of the complexation of boron acids with catechol and substituted catechols, Inorg. Chem 16(7) (1977) 1677–1681.

[25]. Furikado Y, Nagahata T, Okamoto T, Sugaya T, Iwatsuki S, Inamo M, Takagi HD, Odani A, Ishihara K, Universal reaction mechanism of boronic acids with diols in aqueous solution: kinetics and the basic concept of a conditional formation constant, Chem. Eur. J 20(41) (2014) 13194–13202. [PubMed: 25169423]

[26]. Springsteen G, Wang B, A detailed examination of boronic acid–diol complexation, Tetrahedron 58(26) (2002) 5291–5300.

[27]. Narkar AR, Barker B, Clisch M, Jiang J, Lee BP, pH Responsive and Oxidation Resistant Wet Adhesive based on Reversible Catechol-Boronate Complexation, Chemistry of Materials 28(15) (2016) 5432–9. [PubMed: 27551163]

[28]. Narkar AR, Kendrick C, Bellur K, Leftwich T, Zhang Z, Lee BP, Rapidly responsive smart adhesive-coated micropillars utilizing catechol-boronate complexation chemistry, Soft matter 15(27) (2019) 5474–5482. [PubMed: 31237299]

[29]. Su J, Chen F, Cryns VL, Messersmith PB, Catechol polymers for pH-responsive, targeted drug delivery to cancer cells, J. Am. Chem. Soc 133(31) (2011) 11850–11853. [PubMed: 21751810]

[30]. Yu N, Wang X, Qiu L, Cai T, Jiang C, Sun Y, Li Y, Peng H, Xiong H, Bacteria-triggered hyaluronan/AgNPs/gentamicin nanocarrier for synergistic bacteria disinfection and wound healing application, Chem. Eng. J 380 (2020).

[31]. Huang Z, Delparastan P, Burch P, Cheng J, Cao Y, Messersmith PB, Injectable dynamic covalent hydrogels of boronic acid polymers cross-linked by bioactive plant-derived polyphenols, Biomaterials Science 6(9) (2018) 2487–2495. [PubMed: 30069570]

[32]. Khutoryanskaya OV, Mayeva ZA, Mun GA, Khutoryanskiy VV, Designing Temperature-Responsive Biocompatible Copolymers and Hydrogels Based on 2-Hydroxyethyl(meth)acrylates, Biomacromol 9(12) (2008) 3353–3361.

[33]. Liu Y, Lee BP, Recovery property of double-network hydrogel containing a mussel-inspired adhesive moiety and nano-silicate, Journal of Materials Chemistry B 4(40) (2016) 6534–6540. [PubMed: 28461887]

[34]. Narkar AR, Kelley JD, Pinnaratip R, Lee BP, Effect of Ionic Functional Groups on the Oxidation State and Interfacial Binding Property of Catechol-Based Adhesive, Biomacromol 19(5) (2018) 1416–1424.

[35]. Bhuiyan MSA, Liu B, Manuel J, Zhao B, Lee BP, Effect of Conductivity on In Situ Deactivation of Catechol–Boronate Complexation-Based Reversible Smart Adhesive, Biomacromol 22(9) (2021) 4004–4015.

[36]. Van Duin M, Peters JA, Kieboom APG, Van Bekkum H, Studies on borate esters 1: The ph dependence of the stability of esters of boric acid and borate in aqueous medium as studied by 11B NMR, Tetrahedron 40(15) (1984) 2901–2911.

[37]. Sienkiewicz PA, Roberts DC, Chemical affinity systems—I: pH dependence of boronic acid-diol affinity in aqueous solution, J. Inorg. Nucl. Chem 42(11) (1980) 1559–1575.

[38]. Yan J, Springsteen G, Deeter S, Wang B, The relationship among pKa, pH, and binding constants in the interactions between boronic acids and diols—it is not as simple as it appears, Tetrahedron 60(49) (2004) 11205–11209.

[39]. Stavitskaya A, Batasheva S, Vinokurov V, Fakhrullina G, Sangarov V, Lvov Y, Fakhrullin R, Antimicrobial applications of clay nanotube-based composites, Nanomaterials 9 (2019) 708.

[40]. Li Y, Meng H, Liu Y, Narkar A, Lee BP, Gelatin microgel incorporated poly(ethylene glycol)-based bioadhesive with enhanced adhesive property and bioactivity, ACS Appl. Mater. Interfaces 8(19) (2016) 11980–11989. [PubMed: 27111631]

[41]. Li Y, Meng H, Liu Y, Narkar A, Lee BP, Gelatin Microgel Incorporated Poly(ethylene glycol)-Based Bioadhesive with Enhanced Adhesive Property and Bioactivity, ACS Appl. Mater. Interfaces 8(19) (2016) 11980–9. [PubMed: 27111631]

[42]. Skelton S, Bostwick M, O'Connor K, Konst S, Casey S, Lee BP, Biomimetic adhesive containing nanocomposite hydrogel with enhanced materials properties, Soft Matter 9(14) (2013) 3825–3833.

[43]. Suzuki Y, Kusuyama D, Sugaya T, Iwatsuki S, Inamo M, Takagi HD, Ishihara K, Reactivity of Boronic Acids toward Catechols in Aqueous Solution, The Journal of Organic Chemistry 85(8) (2020) 5255–5264. [PubMed: 32003994]

[44]. Park E-S, Moon W-S, Song M-J, Kim M-N, Chung K-H, Yoon J-S, Antimicrobial activity of phenol and benzoic acid derivatives, Int. Biodeterior. Biodegrad 47(4) (2001) 209–214.

[45]. Heath RJ, Yu YT, Shapiro MA, Olson E, Rock CO, Broad spectrum antimicrobial biocides target the FabI component of fatty acid synthesis, J. Biol. Chem 273(46) (1998) 30316–30320. [PubMed: 9804793]

[46]. Lana EJL, Carazza F, Takahashi JA, Antibacterial evaluation of 1,4-benzoquinone derivatives, J. Agric. Food Chem 54(6) (2006) 2053–2056. [PubMed: 16536574]

[47]. Carcamo-Noriega EN, Sathyamoorthi S, Banerjee S, Gnanamani E, Mendoza-Trujillo M, Mata-Espinosa D, Hernández-Pando R, Veytia-Bucheli JI, Possani LD, Zare RN, 1,4-Benzoquinone antimicrobial agents against Staphylococcus aureus and Mycobacterium tuberculosis derived from scorpion venom, P. Natl. Acad. Sci. USA 116(26) (2019) 12642.

[48]. Neilson AH, Allard AS, Hynning PÅ, Remberger M, Distribution, fate and persistence of organochlorine compounds formed during production of bleached pulp, Toxicol. Environ. Chem 30(1–2) (1991) 3–41.

[49]. O'Brien PJ, Molecular mechanisms of quinone cytotoxicity, Chem. Biol. Interact 80(1) (1991) 1–41. [PubMed: 1913977]

[50]. Mulder M, Crosier J, Dunn R, Cauda Equina Compression by Hydrogel Dural Sealant After a Laminotomy and Discectomy Case Report, Spine 34(4) (2009) E144–E148. [PubMed: 19214084]

[51]. Blackburn SL, Smyth MD, Hydrogel-induced cervicomedullary compression after posterior fossa decompression for Chiari malformation - Case report, J. Neurosurg 106(4) (2007) 302–304. [PubMed: 17465365]

[52]. Narkar AR, Lee BP, Incorporation of Anionic Monomer to Tune the Reversible Catechol-Boronate Complex for pH-Responsive, Reversible Adhesion, Langmuir 34(32) (2018) 9410–9417. [PubMed: 30032614]

[53]. Gan D, Xing W, Jiang L, Fang J, Zhao C, Ren F, Fang L, Wang K, Lu X, Plant-inspired adhesive and tough hydrogel based on Ag-Lignin nanoparticles-triggered dynamic redox catechol chemistry, Nature communications 10(1) (2019) 1–10.

[54]. Gan D, Xu T, Xing W, Ge X, Fang L, Wang K, Ren F, Lu X, Mussel-inspired contact-active antibacterial hydrogel with high cell affinity, toughness, and recoverability, Advanced Functional Materials 29(1) (2019) 1805964.

[55]. Li X, Wu B, Chen H, Nan K, Jin Y, Sun L, Wang B, Recent developments in smart antibacterial surfaces to inhibit biofilm formation and bacterial infections, J. Mater. Chem. B 6(26) (2018) 4274–4292. [PubMed: 32254504]

[56]. Cheng G, Xue H, Zhang Z, Chen S, Jiang S, A switchable biocompatible polymer surface with self-sterilizing and nonfouling capabilities, Angew. Chem. Int. Edit 47(46) (2008) 8831–8834.

[57]. Xiong M, Bao Y, Xu X, Wang H, Han Z, Wang Z, Liu Y, Huang S, Song Z, Chen J, Peek RM, Yin L, Chen L-F, Cheng J, Selective killing of Helicobacter pylori with pH-responsive helix-coil conformation transitionable antimicrobial polypeptides, P. Natl. Acad. Sci. USA 114(48) (2017) 12675.

[58]. Tague AJ, Putsathit P, Hammer KA, Wales SM, Knight DR, Riley TV, Keller PA, Pyne SG, Cationic biaryl 1,2,3-triazolyl peptidomimetic amphiphiles: synthesis, antibacterial evaluation and preliminary mechanism of action studies, European Journal of Medicinal Chemistry 168 (2019) 386–404. [PubMed: 30831407]

[59]. Montanari E, Gennari A, Pelliccia M, Gourmel C, Lallana E, Matricardi P, McBain AJ, Tirelli N, Hyaluronan/tannic acid nanoparticles via catechol/boronate complexation as a smart antibacterial system, Macromol. Biosci 16(12) (2016) 1815–1823. [PubMed: 27735135]

Highlights

- Bacterial infection is associated with acidic microenvironment
- pH responsive hydrogel consisted of chlorinated catechol and phenylboronic acid
- Catechol-boronate complex formed and dissociated reversibly with pH
- Hydrogel demonstrated pH dependent antibacterial activity
- Cytotoxicity of hydrogel can be attenuated by pH

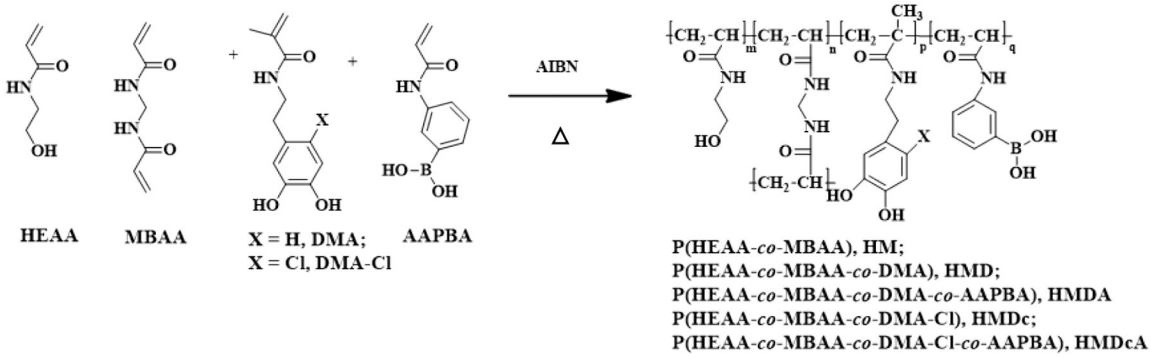

Figure 1.
Synthesis of hydrogels.

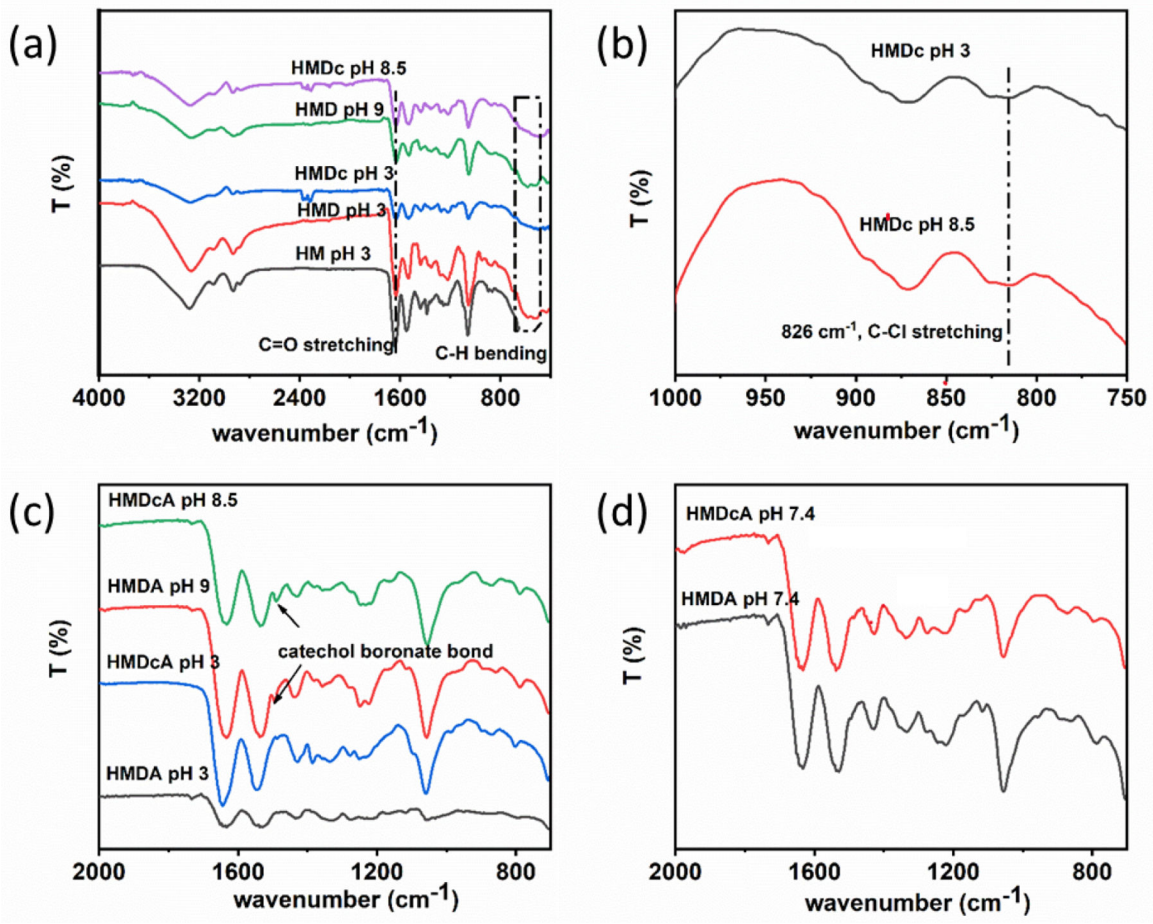

Figure 2.

FTIR spectra of (a) HM, HMD, and HMDc at pH 3, 8.5 and 9, (b) HMDc at pH 3 and 8.5 from 1000 to 750 cm^{-1}, (c) HMDA and HMDcA at pH 3, 8.5 and 9, (d) HMDA and HMDcA at pH 7.4.

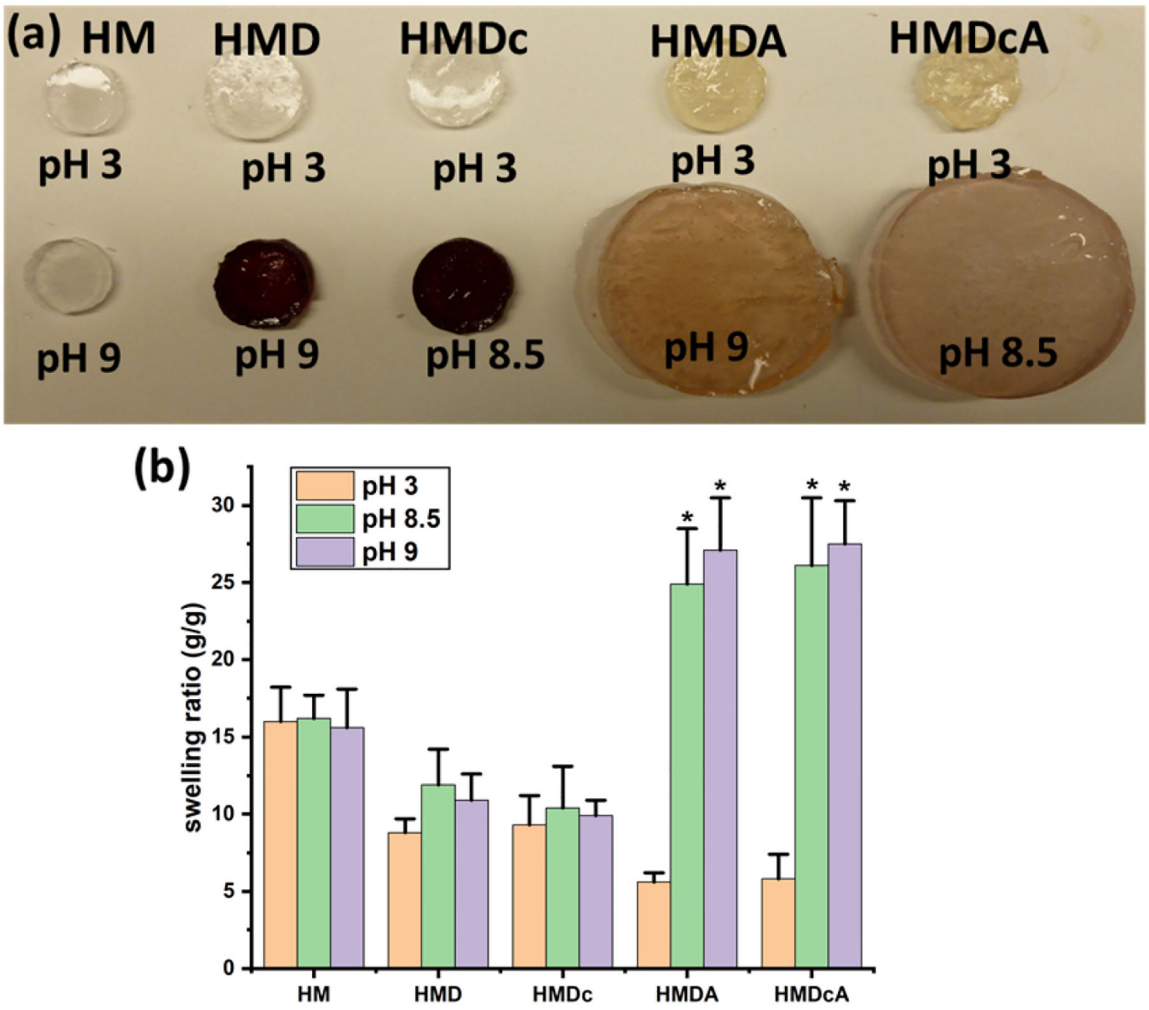

Figure 3.

(a) Optical images of hydrogels after incubation at pH 3, pH 8.5 and pH 9 for 24 h, (b) Swelling ratios of HM, HMD, HMDc, HMDA and HMDcA at pH 3, 8.5 and 9. *$p < 0.05$ when compared to the hydrogel incubated at pH 3 for a given composition.

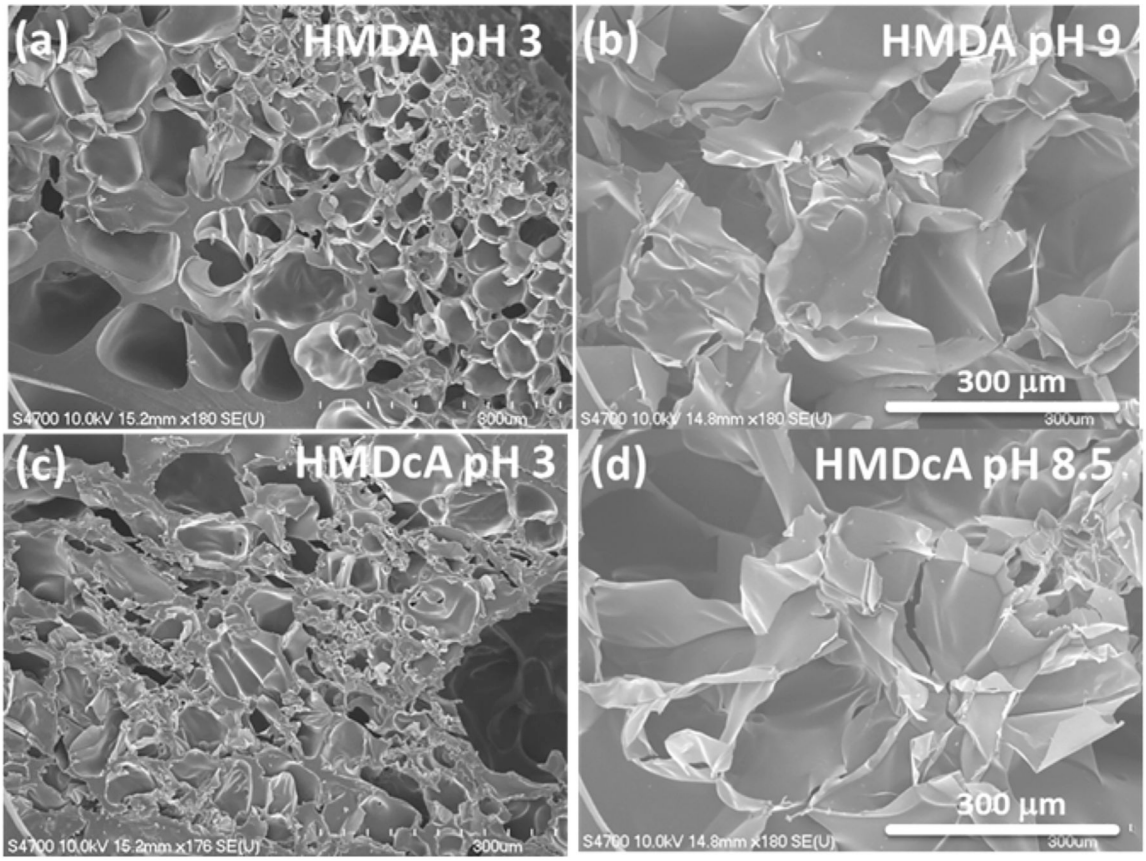

Figure 4.

SEM images of lyophilized HMDA after incubation at (a) pH 3 and (b) pH 9 for 24 h and images of lyophilized HMDcA after incubation at (c) pH 3 and (d) pH 8.5 for 24 h. Scale bar = 300 µm.

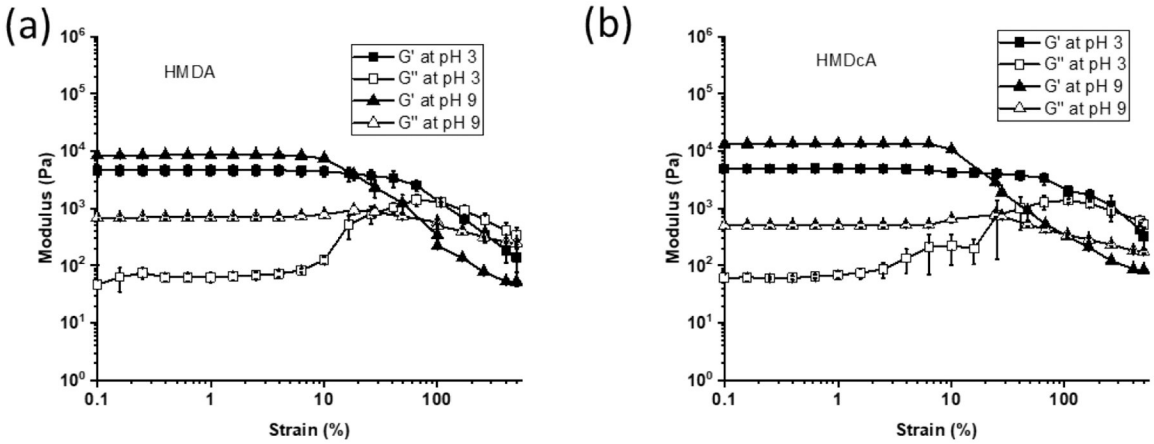

Figure 5.

G′ (filled symbol) and G″ (open symbol) for (a) HMDA and (b) HMDcA equilibrated at different pH.

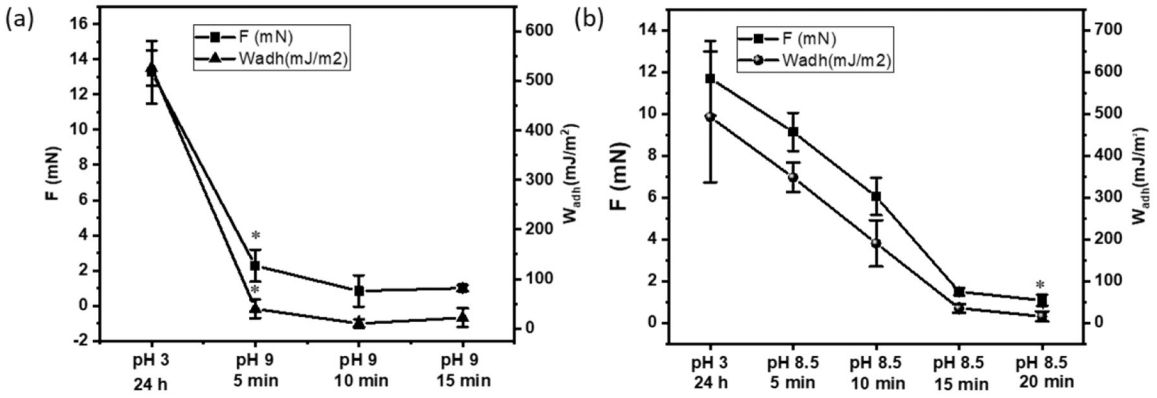

Figure 6.

Average F_{max} and W_{adh} values for (a) HMDA and (b) HMDcA hydrogels brought in contact with a borosilicate glass surface after they were equilibrated a basic pH (pH 9 and 8.5 for HMDA and NMDcA, respectively) for up to 20 min. Contact mechanic testing was perform using an interfacial buffer with the same pH. *$p < 0.05$ when compared to the hydrogel incubated at pH 3 for a given composition.

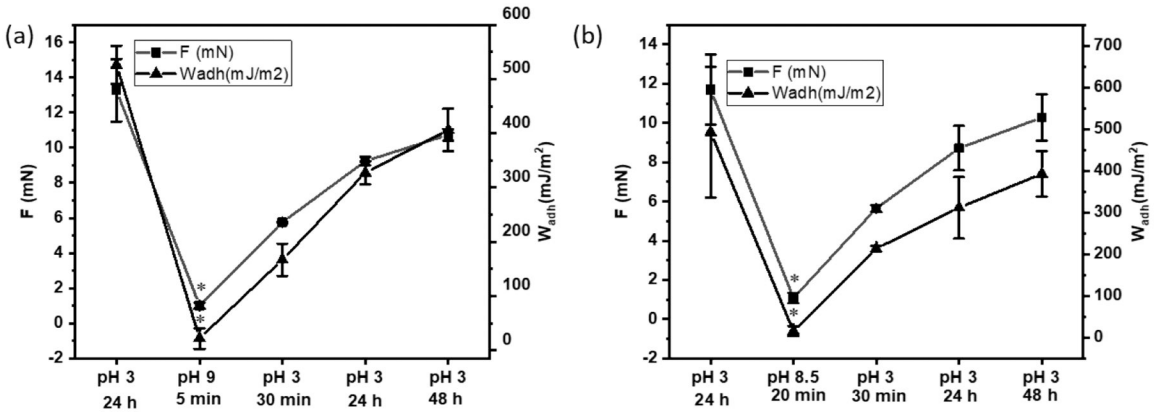

Figure 7.

Average F_{max} and W_{adh} values for (a) HMDA and (b) HMDcA hydrogel brought into successive contacts with a borosilicate glass after equilibration at pH 3 (1st contact), basic pH (2nd contact at pH 9 and 8.5 for HMDA and HMDcA, respectively) and finally at pH 3 for up to 48 h. Contact mechanic testing was perform using an interfacial buffer with the same pH. *$p < 0.05$ when compared to the hydrogel incubated at pH 3 for a given composition.

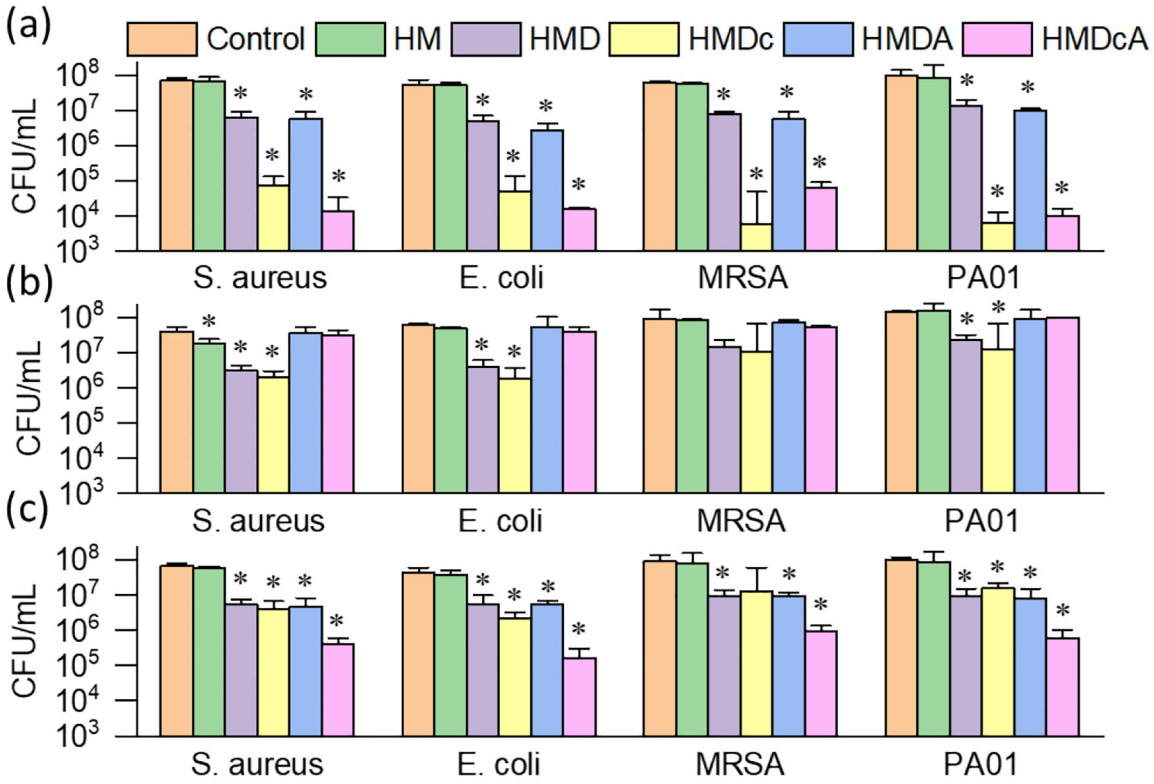

Figure 8.

Antibacterial activity of hydrogels. CFU count of bacteria after treatment of hydrogels incubated at (a) pH 3, (b) pH 8.5 (HMDc and HMDcA), at pH 9 (HM, HMD and HMDA), (c) pH 8.5, then pH 3 (HMDc and HMDcA); pH 9, then at pH 3 (HM, HMD and HMDA). *$p < 0.05$ when compared to the untreated control sample at the given pH.

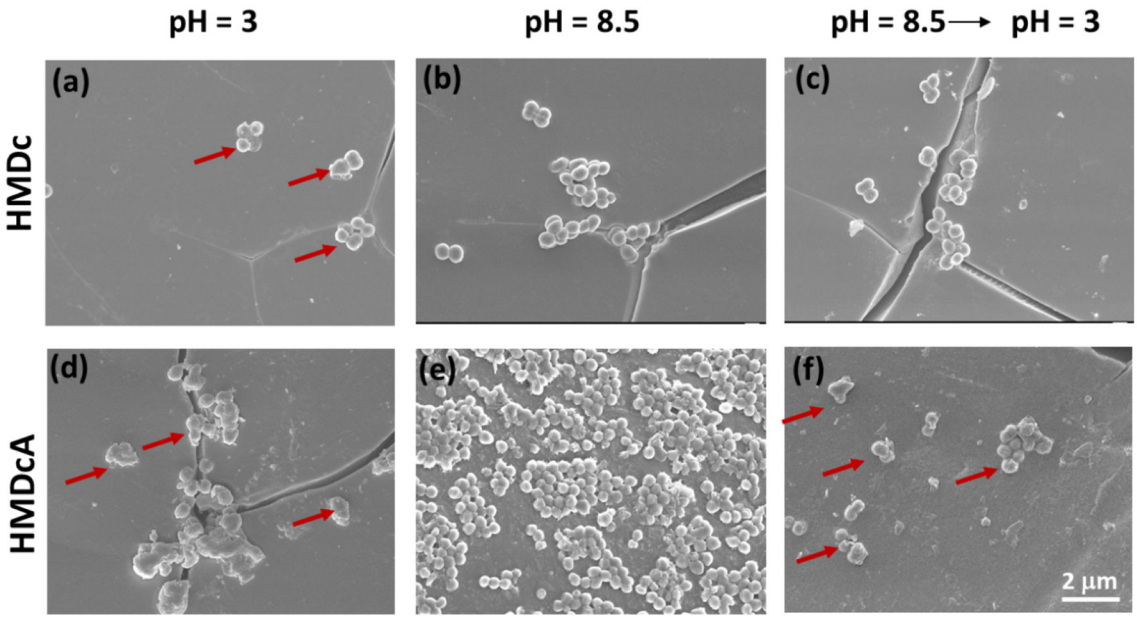

Figure 9.

FE-SEM images of MRSA applied over the surface of HMDc that was previously incubated at (a) pH 3 for 24 h, (b) pH 8.5 for 12 h, (c) first pH 8.5 for 12 h, then pH 3 for 24 h, and HMDcA that was previously incubated at (d) pH 3 for 24 h, (e) pH 8.5 for 12 h, (f) first pH 8.5 for 12 h, then pH 3 for 24 h. The red arrows indicated the morphology change of bacteria. Scale bar= 2 μm.

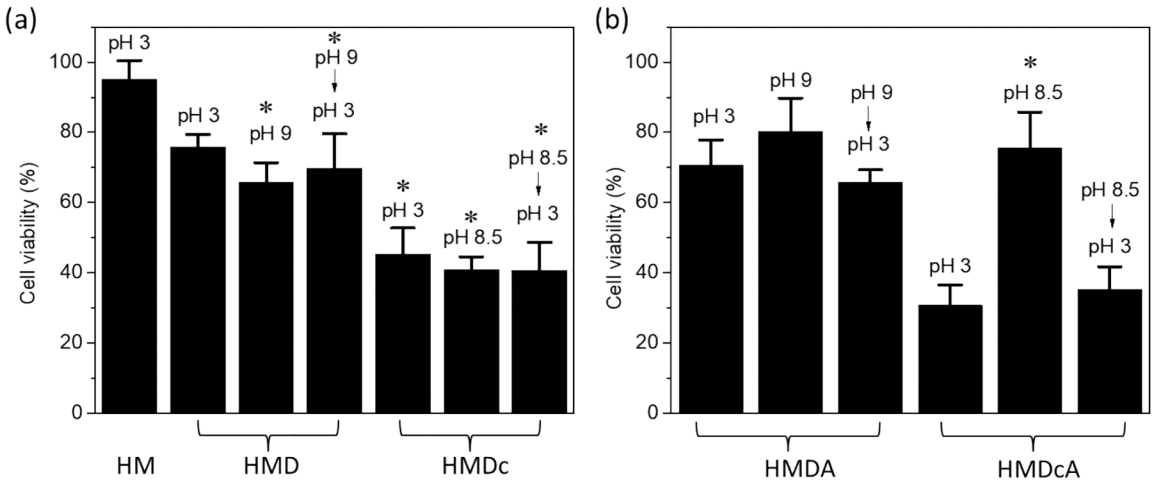

Figure 10.

Cell viability of HSF incubated with (a) HM (treated in pH 3), HMD, and HMDc and (b) HMDA and HMDcA hydrogels. Hydrogels were treated first with pH 3, pH 9 (HMD and HMDA) or 8.5 (HMDA and HMDcA), and then pH 3 before cytotoxicity testing. *$p < 0.05$ when compared to HM incubated at pH 3. **$p < 0.05$ when compared to HMDcA incubated at pH 3.